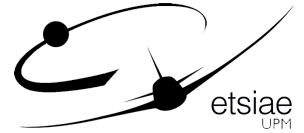




UNIVERSIDAD
POLITÉCNICA
DE MADRID



UNIVERSIDAD POLITÉCNICA DE MADRID

ESCUELA TÉCNICA SUPERIOR DE INGENIERÍA

AERONÁUTICA Y DEL ESPACIO

GRADO EN INGENIERÍA AEROESPACIAL

TRABAJO FIN DE GRADO

Modelización y simulación del crecimiento de hielo en superficies.

AUTOR: Rodrigo Fernández Matilla

ESPECIALIDAD: Ciencias y Tecnologías Aeroespaciales

TUTOR PROFESIONAL: Mariola Gómez López

TUTOR ACADÉMICO: Marta Cordero Gracia

Junio 2020

Contents

Nomenclature	v
A Absolute and relative orbital element sets.	1
A.1 Introduction.	1
A.2 Absolute element sets.	1
A.2.1 Workflow for transformations between absolute element sets.	1
A.2.2 Element sets.	2
A.3 Relative sets.	6
A.3.1 Workflow for transformations between ROEs.	6
A.3.2 Element sets.	9
B Cartesian reference systems.	13
B.1 Introduction.	13
B.1.1 Inertial and rotating reference frames.	13
B.1.2 Absolute and relative frames.	13
B.1.3 Time measurement.	14
B.2 Absolute reference systems.	14
B.2.1 Earth-Centered-Inertial reference system (ECI).	14
B.2.2 Earth-Centered, Earth-Fixed reference system (ECEF).	15
B.2.3 Perifocal (PQW) reference frame.	19
B.3 Relative reference systems.	22
B.3.1 LVLH reference frame.	22
B.3.2 RTN reference frame.	23
B.3.3 TAN reference frame.	23
B.4 Conversions from OEs to cartesian coordinates.	23
B.4.1 ECI to Keplerian OEs and vice versa.	23
B.4.2 Relative Keplerian OEs to LVLH.	23
Bibliography	25
General	25

Eccentric Dynamics	26
Perturbations	26
MATLAB Exchange libraries	27

Nomenclature

Physical constants

γ Coeficiente de dilatación adiabática de un gas $[-]$

T_C Temperatura del punto triple $[K]$

\mathbf{A} Matriz de autovalores de un sistema de ecuaciones diferenciales

λ_i Autovalor i -ésimo de la matriz del sistema

\mathbf{A} Matriz del sistema de una ecuación diferencial

$\mathbf{F}(\mathbf{U})$ Vector de flujos de una ecuación diferencial

\mathbf{I} Matriz identidad

$\mathbf{K}^{(i)}$ Autovector i -ésimo de la matriz del sistema

\mathbf{n} Vector normal exterior a una superficie

\mathbf{R} Vector de términos fuente de una ecuación diferencial

\mathbf{U} Vector de variables dependientes de un sistema de ecuaciones diferenciales

\mathbf{U} Vector de variables dependientes de una ecuación diferencial

\mathbf{W} Vector de variables dependientes canónicas de un sistema de ecuaciones diferenciales

\mathbb{I} Unidad imaginaria

$\mathcal{L}(\mathbf{U})$ Operador diferencial espacial de una ecuación diferencial en derivadas parciales

Ω Volumen geométrico

$\partial\Omega$ Frontera del volumen Ω

ϕ Superficie característica de una ecuación diferencial en derivadas parciales

Σ Superficie geométrica

$d\gamma, d\sigma, d\omega$ Diferenciales de arco, superficie y volumen

s Parámetro de longitud de arco

Cartesian coordinates

\bar{u}_i^n Solución exacta de un esquema numérico

$F_{i+1/2}$ Flujos numéricos en el extremo superior del volumen finito i -ésimo

Q Vector de parámetros del método de Roe

$U_{i+1/2}$ Solución computada en el extremo superior del volumen finito i -ésimo

$\Delta x, \Delta t$ Pasos espacial y temporal

ϵ_T Error de truncamiento de un esquema numérico

λ_j Longitud de onda del armónico j -ésimo

ω Relación de dispersión numérica

Ω_i Volumen de control i -ésimo

ϕ_j Fase del armónico j -ésimo

σ Número CFL

$\tilde{\mathbf{A}}$ Matriz promediada del sistema

$\tilde{\lambda}_i$ Autovalor i -ésimo de la matriz promediada del sistema

$\tilde{\omega}$ Relación de dispersión

$\tilde{K}^{(i)}$ Autovector i -ésimo de la matriz promediada del sistema

\tilde{u}_i^n Solución exacta de un modelo matemático

G_j Factor de amplificación o ganancia del armónico j -ésimo

I_i Centroides del volumen finito i -ésimo

k_j Número de onda del armónico j -ésimo

$N(\bullet)$ Esquema numérico

S	Velocidad de propagación de una discontinuidad
S_{max}^n	Velocidad máxima de propagación de información en un problema de evolución discretizado
u_i^n	Solución computada de un esquema numérico
V_j^n	Amplitud del armónico j -ésimo en el instante n -ésimo
$x_{i+1/2}$	Extremo superior del volumen finito i -ésimo

Characteristic numbers

Fr	Número de Froude	$Fr = \frac{U_c}{\sqrt{g_0 L_c}}$
Nu	Número de Nusselt	$Nu = \frac{h_c L_c}{k}$
Pr	Número de Prandtl	$Pr = \frac{\nu}{\alpha}$
Re	Número de Reynolds	$Re = \frac{\rho_c U_c L_c}{\mu_c}$

Suffixes

∞	Variable en el infinito sin perturbar
c	Característica
d	Gota (<i>droplet</i>)
e	Borde de la capa límite (<i>edge</i>)
f	Película de agua (<i>water film</i>)
w	Agua (<i>water</i>)

Orbital elements

α	Difusividad térmica	$\left[\frac{m^2}{s} \right]$
α_w	Fracción volumétrica de agua en aire	$[- - -]$
\bar{U}	Vector velocidad de un cuerpo o fluido	$\left[\frac{m}{s} \right]$
\bar{u}	Vector velocidad adimensional de un cuerpo o fluido	$[- - -]$

β	Coeficiente de captación	$[- - -]$
\dot{m}	Flujo másico	$\left[\frac{kg}{s} \right]$
\dot{m}'	Flujo másico por unidad de área	$\left[\frac{kg}{s} \frac{1}{m^2} \right]$
\dot{Q}	Flujo de calor $[W]$	
\dot{q}	Flujo de calor por unidad de área	$\left[\frac{W}{m^2} \right]$
μ	Viscosidad dinámica de un fluido	$[Pa \cdot s]$
ν	Viscosidad cinemática de un fluido	$\left[\frac{m^2}{s} \right]$
$\bar{\tau}_{wall}$	Esfuerzo viscoso de un fluido sobre una pared	$[Pa]$
\bar{c}_f	Coeficiente de fricción viscosa sobre una pared	$[- - -]$
ρ	Densidad de un fluido	$\left[\frac{kg}{m^3} \right]$
θ	Temperatura absoluta adimensionalizada con la del punto triple	$[- - -]$
\tilde{T}	Temperatura	$[C]$
C_D	Coeficiente de resistencia de un cuerpo	$[- - -]$
C_p	Calor específico a presión constante	$\left[\frac{J}{kg K} \right]$
d	Diámetro de las gotas	$[\mu m]$
f	Fracción de agua congelada	$[- - -]$
h	Espesor de una película de agua	$[m]$
h_c	Coeficiente de transferencia de calor por convección	$\left[\frac{W}{m^2 K} \right]$
k	Conductividad térmica de un fluido	$\left[\frac{W}{m K} \right]$
L	Calor latente de un fluido	$\left[\frac{J}{kg} \right]$
LWC	Contenido en agua líquida, <i>liquid water content</i>	$\left[\frac{kg}{m^3} \right]$
MVD	Tamaño volumétrico medio de las gotas, <i>median volumetric diameter</i>	$[\mu m]$

p	Presión de un fluido	$[Pa]$
$p_{v,sat}$	Presión de vapor de saturación	$[Pa]$
r	Factor de recuperación adiabática	$[- - -]$
T	Temperatura absoluta	$[K]$

List of Figures

A.1	Workflow for transforming between two arbitrary absolute element sets.	2
A.2	Frame rotation from inertial to perifocal frame.	3
A.3	Workflow for transforming any relative set into KOE.	8
A.4	Workflow for transforming RKOE into any other set.	9
A.5	Relative ccentricity & inclination vectors.	10

List of Tables

Absolute and relative orbital element sets.

A.1 Introduction.

The description of a spacecraft's state is done via a **state vector**. While it can include several variables with other purposes (*e.g.* filtering), its only information throughout this thesis is the position and velocity. There are two main ways to describe them:

- A. Through cartesian coordinates
- B. Through orbital elements

While the first option yields a very explicit and graphic-ready description, the second one usually has two advantages over it. Firstly, orbital elements are generally more intuitive about both the orbit and the position on it. Secondly, as orbital elements are generally slow-varying, they allow for a bigger integration timestep without losing accuracy. This is quite clear when studying keplerian motion, as most of the elements remain constant. Variational formulation and Hamilton-Jacobi theory (with the notion of changing variables as the full solution of a problem) relate to this fact.

Throughout this thesis, several sets of orbital elements have been used. The goal of this appendix is to clarify on the definition and differences between them. Absolute orbital elements (OEs) will be described first, followed by relative OEs (ROEs).

A.2 Absolute element sets.

A.2.1 Workflow for transformations between absolute element sets.

Consider two different sets of OEs, denoted by \underline{OE} and $\widetilde{\underline{OE}}$. The transformation function $\mathbf{G}_{OE \rightarrow \widetilde{OE}}$ between them is defined by:

$$\widetilde{\underline{OE}} = \mathbf{G}_{OE \rightarrow \widetilde{OE}}(\underline{OE}) \tag{A.1}$$

A numerous amount of element sets have been historically defined. Nevertheless, some of them are much more commonly used than others. Although we will restrain ourselves to a short number of sets (say n), the number of transformations becomes arduously large as n increases ($n(n-1)$).

In order to reduce the number of transformation functions \mathbf{G} , let us use the later defined Keplerian OEs (KOE) as a pivot, that is, building only transformations to and from KOEs. This will in turn reduce the number of required functions to $2n$. The Keplerian set also has a further advantage: as it is the classical element set, almost every other set is defined explicitly in terms of it, so that transformations to and from them can easily be derived. A simple, graphical explanation of this is shown in figure A.1.



Figure A.1: Workflow for transforming between two arbitrary absolute element sets.

A.2.2 Element sets.

A.2.2.1 Keplerian orbital elements (KOE).

The Keplerian set of OEs (KOE) is one of the most widely used and classic options. While the last element may change from author to author, an usual definition is the following:

$$\left\{ \begin{array}{lll} a & \equiv & \text{Semimajor axis} & [L] \\ e & \equiv & \text{Eccentricity} & [--] \\ i & \equiv & \text{Inclination} & [rad] \\ \Omega \text{ or } RAAN & \equiv & \text{Right ascension of the ascending node} & [rad] \\ \omega & \equiv & \text{Argument of periapsis} & [rad] \\ M & \equiv & \text{Mean anomaly} & [rad] \end{array} \right. \quad (\text{A.2})$$

The last element commonly varies across literature, being substituted by the true anomaly θ ; or, when tackling the variation of orbital parameters, by the mean anomaly at $t = 0$ (M_0) or the perigee time T_0 [1]. Mean anomaly is used due to the simplicity of its unperturbed variational equation, as it has a constant rate (denoted by n). The geometrical meaning and definition of these elements is out from the scope of this thesis. Nonetheless, figure A.2 shows a simple geometrical drawing of the involved angles.

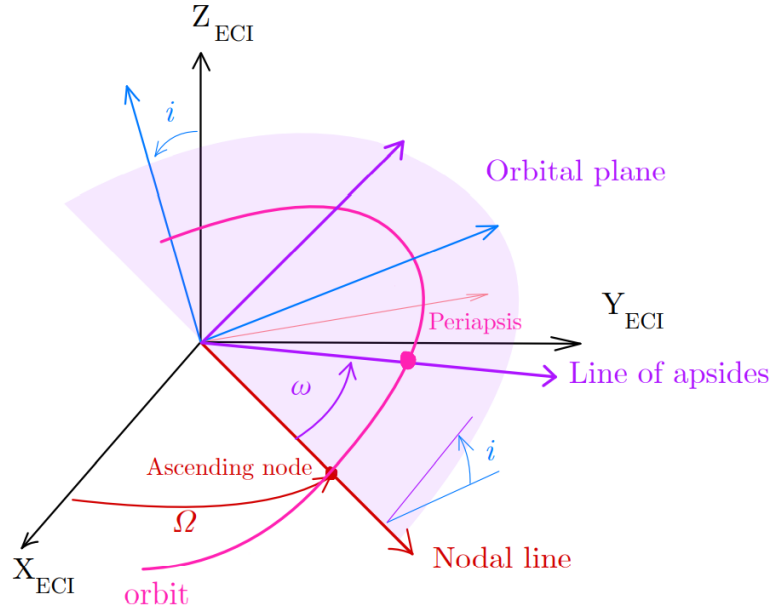


Figure A.2: Frame rotation from inertial to perifocal frame.

As it is seen in the figure before, the Keplerian elements become singular in two cases:

- A. If the **inclination** is null, the orbital plane is coincident with the inertial reference (ECI x-y) plane. The ascending node is hence undefined in this case.
- B. If the **eccentricity** is null, the periapsis is not defined, as it is the nearest point of the orbit around the central body. Thus, there is no angle defining its position, making the argument of periapsis nonsingular.

These singularities are unfortunately quite common in orbit design. They correspond respectively with equatorial and circular orbits. In order to avoid this behaviour, many different elements sets have been defined. Wiesel [1] shows an intuitive approach in chapter 2.10, solving either problem with a graphic approach.

A.2.2.2 Eccentricity/inclination vectors orbital elements (EIOE).

This set, originally defined for geostationary orbits in absolute terms [2], is used mainly as a relative OE set. Though it is actually not used along this thesis, its definition is helpful for introducing the common relative counterpart. In any case, let us proceed with the eccentricity and inclination vectors concept.

Eccentricity vector

The notion of the eccentricity vector is quite basic, as it is, when in unperturbed motion, a constant of the dynamic system. It is defined as the eccentricity-sized vector pointing towards the perigee. Nonetheless, for this purpose, the eccentricity vector is defined as [3]:

$$\underline{e} = \begin{Bmatrix} e_x \\ e_y \end{Bmatrix} = e \begin{Bmatrix} \cos \varpi \\ \sin \varpi \end{Bmatrix} \quad (\text{A.3})$$

where the argument of perigee ω might be substituted with the sum $\omega + \Omega$ [as in 2]. A graphical representation can be seen later in the relative definition A.5(a). As it arises from (A.3), it substitutes the eccentricity and argument of perigee from the Keplerian OE set.

Inclination vector

The inclination vector is perpendicular to the orbital plane, similarly to the angular momentum, but inclination-sized. It is defined by its components as [2]:

$$\underline{i} = \begin{Bmatrix} i_x \\ i_y \end{Bmatrix} = i \begin{Bmatrix} \cos \Omega \\ \sin \Omega \end{Bmatrix}$$

The graphical interpretation is not as straightforward as for the eccentricity vector. Nonetheless, we are only interested in the definition itself. It is clear that this components substitute the out-of-plane related elements i and Ω .

Element set

The EI orbital element set is then composed of:

$$\left\{ \begin{array}{lll} a & \equiv & \text{Semimajor axis} \quad [L] \\ e_x = e \cos \omega & \equiv & \text{x-projection of } \underline{e} \quad [--] \\ e_y = e \sin \omega & \equiv & \text{y-projection of } \underline{e} \quad [--] \\ i_x & \equiv & \text{x-component of } \underline{i} \quad [--] \\ i_y & \equiv & \text{y-component of } \underline{i} \quad [--] \\ \lambda = \omega + M & \equiv & \text{Mean argument of latitude} \quad [rad] \end{array} \right. \quad (\text{A.4})$$

A.2.2.3 Quasi-nonsingular orbital elements (QNSOE).

The quasi-nonsingular (QNS) orbital element set tackles the singularity existing in circular orbits [4], [5] [6]. It is quite similar to the formerly defined EI set, as it uses again the components of the eccentricity vector to substitute e and ω . The set is then defined as:

$$\left\{ \begin{array}{lll} a & \equiv & \text{Semimajor axis} & [L] \\ q_1 = e \cos \omega & \equiv & \text{x-projection of } \underline{e} & [---] \\ q_2 = e \sin \omega & \equiv & \text{y-projection of } \underline{e} & [---] \\ i & \equiv & \text{Inclination} & [rad] \\ \Omega & \equiv & \text{Right ascension of the ascending node} & [rad] \\ u = \omega + \theta & \equiv & \text{True argument of latitude} & [rad] \end{array} \right. \quad (\text{A.5})$$

Though some authors use a different order, this is the one used in this thesis, so as to keep the time-varying element on the last place.

A.2.2.4 Equinoctial orbital elements (EOE).

The QNS set of elements only solved half of the singularity problem. To solve both, thus enabling the description of equatorial and polar orbits, the equinoctial set of elements is defined as:

$$\left\{ \begin{array}{lll} a & \equiv & \text{Semimajor axis} & [L] \\ P_1 = e \cos \varpi & \equiv & \text{unclear physical meaning, similar to } e_x & [---] \\ P_2 = e \sin \varpi & \equiv & \text{unclear physical meaning, similar to } e_y & [---] \\ Q_1 = \tan \frac{i}{2} \cos \Omega & \equiv & \text{unclear physical meaning, similar to } i_x & [---] \\ Q_2 = \tan \frac{i}{2} \sin \Omega & \equiv & \text{unclear physical meaning, similar to } i_y & [---] \\ L = \Omega + \omega + \theta & \equiv & \text{True longitude} & [rad] \end{array} \right. \quad (\text{A.6})$$

Not only does the order does change depending on the author, but also the symbols to refer to them. An example of its use is [4].

A.2.2.5 Delaunay orbital elements (DOE).

Delaunay elements arise when formulating the two-body problem through analytical mechanics. All of the previous element sets are clearly non-canonical (*i.e.* they do not satisfy Hamilton's equations). Starting from the canonical set of elements (see appendix **PUT APPENDIX**), Delaunay elements

are reached after performing a canonical transformation, leading to the following definition:

$$\left\{ \begin{array}{lll} L = \sqrt{\mu a} & \equiv & \text{unclear physical meaning} \quad [L^{1/2}] \\ G = L\sqrt{1 - e^2} & \equiv & \text{Angular momentum} \quad [L^{1/2}] \\ H = G \cos i & \equiv & \text{Polar component of angular momentum} \quad [L^{1/2}] \\ l = M & \equiv & \text{Mean anomaly} \quad [rad] \\ g = \omega & \equiv & \text{Argument of perigee} \quad [rad] \\ h = \Omega & \equiv & \text{Right ascension of ascending node} \quad [rad] \end{array} \right. \quad (\text{A.7})$$

This set is mainly used in the context of perturbations, as it yields a very convenient expression for the perturbed Hamiltonian (see section **PUT SECTION HERE**).

A.3 Relative sets.

Relative elements are at the deepest roots of spacecraft relative motion, offering several advantages over cartesian relative states. First and foremost, they are more intuitive, but they also lead to a reduction of linearisation errors when expanding the deputy's movement around the chief's orbit [7]. In general, relative elements are defined as:

$$\delta \underline{OE} = \mathbf{f}(\underline{OE}_C, \underline{OE}_D) \quad (\text{A.8})$$

which is usually simplified by just taking the arithmetic difference between them, namely

$$\delta \underline{OE} = \underline{OE}_D - \underline{OE}_C \quad (\text{A.9})$$

where the subscripts denote respectively the deputy and chief spacecraft. The question now is, how do transformations between ROEs work.

A.3.1 Workflow for transformations between ROEs.

As for the absolute elements, Keplerian elements will be used as a pivot point. That means that only the transformations from and to RKOE's must be implemented. There are then two types of transformations:

A) From any ROE set to RKOE

While authors provide with scenarios expressed in their own ROE set, the element choice for our simulator is the Keplerian set. That leads us to the need of implementing a transformation from the former set to the latter. Let us assume then the following inputs and outputs:

- **Inputs:**

- $\widetilde{ROE} = \delta\widetilde{OE}$: Different type of ROEs, whose absolute equivalents are known as a function of the KOEs ($\widetilde{OE} = \mathbf{f}(\underline{KOE})$)
- \underline{KOE}_C : Chief spacecraft/reference orbit KOEs

- **Output:**

- $\underline{RKOE} = \delta\underline{KOE}$: Keplerian ROEs

Taking equation (A.9) and particularizing it for KOEs:

$$\delta\underline{KOE} = \underline{KOE}_D - \underline{KOE}_C \quad (\text{A.10})$$

while the second term is known (input), the second one must be calculated through a certain process:

1. Calculate chief's OEs in the source phase space (*i.e.* \widetilde{OE}_C)

$$\widetilde{OE}_C = \mathbf{G}_{KOE \rightarrow \widetilde{OE}}(\underline{KOE}_C)$$

2. Compute deputy's OEs by direct addition

$$\widetilde{OE}_D = \widetilde{OE}_C + \delta\widetilde{OE}$$

3. Compute deputy's KOEs by back-transformation

$$\underline{KOE}_D = \mathbf{G}_{\widetilde{OE} \rightarrow KOE}(\widetilde{OE}_D)$$

4. Subtract chief's KOEs from deputy's

$$\delta\underline{KOE} = \underline{KOE}_D - \underline{KOE}_C$$

See graphic A.3 for a more visual explanation.

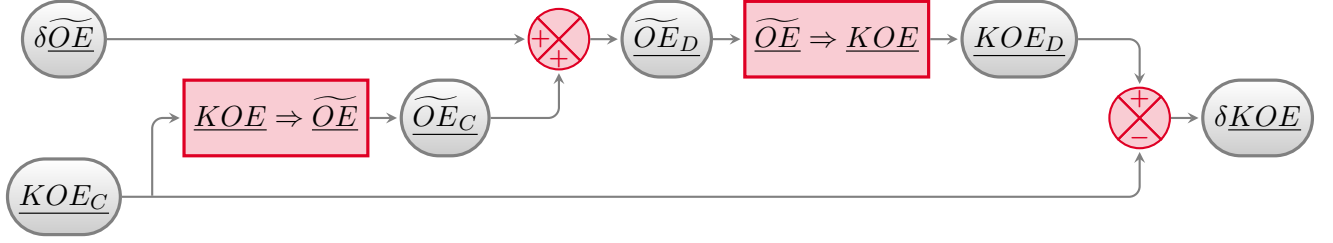


Figure A.3: Workflow for transforming any relative set into KOE.

B) From RKOE to any ROE set

In this case, let us assume the next inputs and outputs:

- **Inputs:**

- $\underline{RKOE} = \underline{\delta KOE}$: Keplerian ROEs
- $\underline{KOE_C}$: Chief KOEs

- **Output:**

- $\underline{ROE} = \underline{\delta OE}$: Different type of ROEs, whose absolute equivalents are known as a function of the KOEs ($\underline{OE} = f(\underline{KOE})$)

For this transformation, the equation A.8 particularized for this case acquires the following shape:

$$\underline{\delta OE} = \underline{OE_D} - \underline{OE_C} \quad (\text{A.11})$$

Equation A.11 can be tackled in two main ways:

- Using the pertinent transformations, compute the absolute elements for both spacecrafts $\underline{OE_D}$, $\underline{OE_C}$, and then calculate the arithmetic difference (in a A.3.1). See graphic A.4.
- Expand the deputy absolute OEs (*i.e.* $\underline{OE_D}$) around the chief via a Taylor series expansion with respect to the Keplerian set of elements, retaining terms up to first order, achieving a linearised expression for the transformation. Mathematically:

$$\underline{OE_D} = \underline{OE}(\underline{KOE_D}) = \underline{OE}(\underline{KOE_C} + \underline{\delta KOE}) = \underline{OE_C} + \frac{\partial \underline{OE}}{\partial \underline{KOE}} \underline{\delta KOE} + \mathcal{O}(\underline{\delta KOE}^2)$$

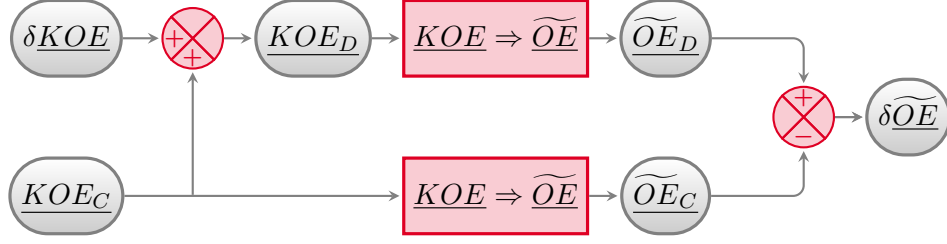


Figure A.4: Workflow for transforming RKOE into any other set.

hence,

$$\delta\widetilde{OE} \approx \widetilde{OE}_C + \frac{\partial\widetilde{OE}}{\partial\widetilde{KOE}}\delta\widetilde{KOE} - \widetilde{OE}_C = \frac{\partial\widetilde{OE}}{\partial\widetilde{KOE}}\delta\widetilde{KOE} \quad (\text{A.12})$$

where the Jacobian matrix is generally simple, as it usually only implies polynomial or trigonometric functions. Equation (A.12) is then a first order approximation of (A.11). Its validity is then reduced to a close proximity between both spacecrafts, which should be assessed.

A.3.2 Element sets.

Besides the ones derived directly from its absolute counterparts, a couple of additional ROE sets will be herewith defined and explained. This is due to one of two reasons. The first one is that some ROE sets are only defined in relative terms, lacking any absolute equivalent. The second one is that it might be interesting to dive in the meaning of the relative sets, deriving interesting relations that would otherwise be overlooked.

A.3.2.1 Eccentricity/inclination vectors relative orbital elements (REIOE).

This ROE set is the counterpart of the EI set (see A.2.2.2). It is nonetheless interesting to see the meaning and shape of it, as it is quite widely used in literature [3, 5, 6]. Let us first define its elements, to later analyze the meaning behind them:

$$\left\{ \begin{array}{lll} \delta a & \equiv & \text{Relative semimajor axis} & [L] \\ \delta e_x & \equiv & \text{Relative x-component of } \underline{e} & [--] \\ \delta e_y & \equiv & \text{Relative y-component of } \underline{e} & [--] \\ \delta i_x & \equiv & \text{Relative x-component of } \underline{i} & [--] \\ \delta i_y & \equiv & \text{Relative y-component of } \underline{i} & [--] \\ \delta \lambda & \equiv & \text{Relative mean argument of latitude} & [rad] \end{array} \right. \quad (\text{A.13})$$

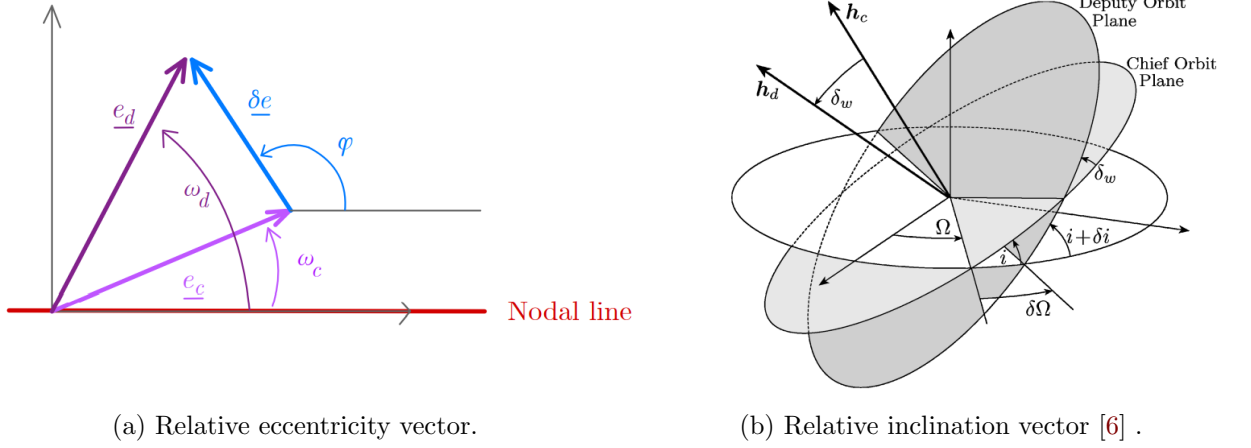


Figure A.5: Relative eccentricity & inclination vectors.

Concept & meaning

The relative eccentricity vector components substitute the relative eccentricity and the relative argument of perigee. It is based on the eccentricity vector definition (A.3), and a graphical representation can be seen in figure A.5(a). Mathematically:

$$\delta \underline{e} = \begin{Bmatrix} \delta e_x \\ \delta e_y \end{Bmatrix} = \delta e \begin{Bmatrix} \cos \varphi \\ \sin \varphi \end{Bmatrix}$$

which rules the in-plane relative motion (hand in hand with δa and $\delta \lambda$). As we know, there are two ways of tackling the transformation from RKOE to this set (see A.3.1). Though the nonlinear form is exact, let us analyze the linear version. If we assume that the difference in the eccentricity vector is due to that of the eccentricity and argument of perigee (δe , $\delta \omega$), we arrive to:

$$\delta \underline{e} \approx \begin{bmatrix} \cos \omega & -e \sin \omega \\ \sin \omega & e \cos \omega \end{bmatrix} \begin{Bmatrix} \delta e \\ \delta \omega \end{Bmatrix} \quad (\text{A.14})$$

where we have neglected terms of second order and higher. The relative inclination vector is defined in an alternative way [3] (comparing with the absolute counterpart). Mathematically:

$$\delta \underline{i} = \sin \delta i \begin{Bmatrix} \cos \theta \\ \sin \theta \end{Bmatrix}$$

where θ is the analog angle to φ in the eccentricity vector. Once again, let us analyze the linearized transformation from RKOE to this set, considering the differences δi and $\delta \Omega$. Applying the law of sines and the law of cosines for spherical trigonometry and assuming small values of δi and $\delta \Omega$, we arrive to:

$$\delta \underline{i} = \begin{Bmatrix} \delta i \\ \sin i \delta \Omega \end{Bmatrix} \approx \begin{bmatrix} 1 & 0 \\ 0 & \sin i \end{bmatrix} \begin{Bmatrix} \delta i \\ \delta \Omega \end{Bmatrix} \quad (\text{A.15})$$

where i is the inclination of the chief's orbit. Combining the results of (A.14) and (A.15) with the definitions of the remaining elements, we can easily arrive to an expression analog to (A.12):

$$\begin{Bmatrix} \delta a \\ \delta e_x \\ \delta e_y \\ \delta i_x \\ \delta i_y \\ \delta \lambda \end{Bmatrix} \approx \begin{bmatrix} 1 & 0 & 0 & 0 & 0 & 0 \\ 0 & \cos \omega & 0 & 0 & -e \sin \omega & 0 \\ 0 & \sin \omega & 0 & 0 & e \cos \omega & 0 \\ 0 & 0 & 1 & 0 & 0 & 0 \\ 0 & 0 & 0 & \sin i & 0 & 0 \\ 0 & 0 & 0 & 0 & 1 & 1 \end{bmatrix} \begin{Bmatrix} \delta a \\ \delta e \\ \delta i \\ \delta \Omega \\ \delta \omega \\ \delta M \end{Bmatrix} \quad (\text{A.16})$$

A graphical representation of this concept can be seen in figure A.5(b).

A.3.2.2 Peters-Noomen C set of relative orbital elements (CROE).

Defined by Peters & Noomen in [8], this set is also closely related with the orbit safety notion. It arises from the analysis of the Gauss Variational Equations (GVEs) applied to the relative dynamics between a deputy and a chief spacecraft, when the former performs a cotangential transfer. Without

further ado, let us define them as:

$$\left\{ \begin{array}{llll} C_1 = \delta p = \eta^2 \delta a - 2 a e \delta e & \equiv & \text{Relative parameter of the orbit} & [L] \\ C_2 = e \delta p - p \delta e & \equiv & \text{unclear physical meaning} & [L] \\ C_3 = -e p (\delta \omega + \cos i \delta \Omega) & \equiv & \text{unclear physical meaning} & [L] \\ C_4 = a (\delta \omega + \cos i \delta \Omega + \eta^{-1} \delta M) & \equiv & \text{Modified relative mean longitude} & [L] \\ C_5 = -p (\cos \omega \delta i + \sin i \sin \omega \delta \Omega) & \equiv & \text{unclear physical meaning} & [L] \\ C_6 = p (\sin \omega \delta i - \sin i \cos \omega \delta \Omega) & \equiv & \text{unclear physical meaning} & [L] \end{array} \right. \quad (\text{A.17})$$

For a proper geometrical and conceptual description of the elements, please see [8]. As an introduction, the first four elements essentially determine the in-plane relative motion. C_1 , C_2 & C_3 arise from a very intelligent interpretation of the GVEs, with C_4 completing the element set. On the other hand, elements C_5 and C_6 describe the out-of-plane motion.

Cartesian reference systems.

B.1 Introduction.

Cartesian states are, as mentioned in appendix A, one of the two main alternatives to describe the state of a certain spacecraft (or celestial body). Though orbital elements (OEs) are generally more intuitive and meaningful, these states are quite critical for the description of both absolute and relative motion. Ultimately, and specially considering the latter, we wish to know the relative orientation and linear distance between the involved bodies. During this appendix, a set of absolute and relative reference frames will be described and related via transformations, which have been used time and again along this thesis.

B.1.1 Inertial and rotating reference frames.

Technically, an inertial reference frame is one where Newton's law holds. Effectively, it is a frame which is not object of any acceleration whatsoever. It is then, when interpreted to the letter, an idealization, as there will always be any perturbation which disavows this assumption. Nonetheless, it is usual to neglect said perturbations up to a certain point, thus considering pseudo-inertial reference frames. From now on then, when inertial reference frames are mentioned they will be considered so, even though they are actually not. Along this thesis, both inertial and rotating frames will be considered, each bearing its different advantages and disadvantages.

B.1.2 Absolute and relative frames.

Another distinction that will be made is between absolute and relative frames. In this thesis, absolute frames are those who are centered in the Earth's center of mass, while relative frames are defined with respect to a reference orbit (the chief's generally). Again, they have different scopes, though relations between them need to be developed.

B.1.3 Time measurement.

Later it will be described how Earth's rotational state influences the dynamics of the spacecrafts, due to its non-homogeneous mass distribution. That leads to the need of precisely computing it, which in turn requires the time elapsed since a given epoch. This section intends to briefly describe the most usual conventions for time definition, without diving in technical considerations. For further description, see [9]. These conventions are:

- I. International Atomic Time (TAI): Physical timescale which is calculated through the measurement of cesium radiation. Lacks intuitive meaning, but acts as a ultra-high precision time system and reference for other timescales.
- II. Universal Time (UT1/UT2): Civil time system, which is defined by the right ascension of the mean Sun. It is not a continuous time system, varying as time passes. There are some smoothed versions of UT1, which filters some seasonal variations, thus accounting only for long-term changes.
- III. Coordinated Universal Time (UTC): Civil time system, which is measured with TAI and synchronized with UT1 via leap seconds. This means that the time rate is the one from the atomic counterpart, whereas the 'reference' is set to follow UT1 within 0.9 seconds. If the difference between UTC and UT1 exceeds this value, 1 second is added/subtracted to get within range. It is then a non-continuous time system.
- IV. Terrestrial Time (TT): Civil time system, which is measured with TAI but has a delay with respect to it (32.184 seconds).

Figure **PUT FIGURE** shows more clearly the differences between them.

B.2 Absolute reference systems.

B.2.1 Earth-Centered-Inertial reference system (ECI).

As previously stated, any Earth-centered reference system will in turn be non-inertial. That leads to the need of defining a common baseline, *i.e.* an epoch at which the reference system is known. The chosen epoch is denoted as J2000.0¹, which translates to January 1st, at 12:00:00.000 (midday) in

¹J2000 denotes a reference frame, being analog to ECI. J2000.0 refers to the mentioned epoch.

Julian years [see 9, glossary]. Effectively, the ECI reference system, is geometrically defined as follows [10]:

$$ECI \equiv \left\{ \begin{array}{lll} \text{Origin} & \equiv & \text{Earth's COM} \\ \text{X-axis} & \equiv & \text{Earth's COM} \longrightarrow \text{Mean vernal equinox at epoch J2000.0} \\ \text{Z-axis} & \equiv & \text{Normal to the mean equatorial plane at epoch J2000.0,} \\ & & \text{pointing towards the Northern Hemisphere} \\ \text{Y-axis} & \equiv & \text{Perpendicular to the X and Z axes forming a right-handed system} \end{array} \right.$$

The main reason behind using this system is that it considerably simplifies the dynamics equation of any spacecraft. It is then the most adequate frame on which dynamics can be solved. Furthermore, when considering relative motion, the reference axis are not a critical axis, as we are rather focused on the motion between spacecrafts. On the other hand, this frame is not able to describe the position relative to Earth's surface, thus being useless in communications or visibility analysis.

B.2.2 Earth-Centered, Earth-Fixed reference system (ECEF).

Due to the formerly mentioned concerns, another Earth-centered reference frame must be defined. In this case, that will be ECEF. Geometrically, it is defined as [10]

$$ECEF \equiv \left\{ \begin{array}{lll} \text{Origin} & \equiv & \text{Earth's COM} \\ \text{X-axis} & \equiv & \text{Earth's COM} \longrightarrow \text{Intersection of prime meridian and true equatorial plane} \\ \text{Z-axis} & \equiv & \text{Earth's true angular velocity vector (rotation axis)} \\ \text{Y-axis} & \equiv & \text{Perpendicular to the X and Z axes forming a right-handed system} \end{array} \right.$$

Once defined, it is turn to evaluate how ECI and ECEF frames differ.

B.2.2.1 Conversion from ECI to ECEF.

Decomposition of the conversion.

There are four essential differences between ECI and ECEF frame, due to four motions that ECEF include due to it being fixed to Earth:

1. Precession of the equinoxes.
2. Nutations (small oscillations) of the equinoxes.
3. Earth's rotation around its axis.
4. Spin axis motion.

Each of this motions can be characterized by a rotation to an associated frame. That is, we can decompose the conversion between ECI and ECEF in four rotations, which will now be analyzed.

Involved intermediate frames & rotations.

ECI(J200) to Mean of Date.

The equinoxes rotate at a slow, but relevant rate. That means that the vernal equinox today differs considerably from the one at J2000.0. The Mean of Date (MOD) frame arises from this notion, being defined as [10]:

$$MOD \equiv \begin{cases} \text{X-axis} & \equiv & \text{Earth's COM} \longrightarrow \text{Mean vernal equinox at current epoch} \\ \text{Z-axis} & \equiv & \text{Perpendicular to the mean equatorial plane at current epoch} \\ \text{Y-axis} & \equiv & \text{Perpendicular to the X and Z axes forming a right-handed system} \end{cases}$$

The rotation matrix from J200 to MOD results:

$$R_{ECI \rightarrow MOD} = \begin{bmatrix} C\zeta_A C\theta_A C z_A - S\zeta_A S z_A & -S\zeta_A C\theta_A C z_A - C\zeta_A S z_A & -S\theta_A C z_A \\ C\zeta_A C\theta_A S z_A + S\zeta_A C z_A & -S\zeta_A C\theta_A S z_A + C\zeta_A C z_A & -S\theta_A S z_A \\ C\zeta_A S\theta_A & -S\zeta_A S\theta_A & C\theta_A \end{bmatrix} \quad (\text{B.1})$$

where the precession angles ζ_A , θ_A and z_A are evaluated by:

$$\begin{cases} \zeta_A & = & 2306.2181''t + 0.30188''t^2 + 0.017998''t^3 \\ \theta_A & = & 2004.3109''t - 0.42665''t^2 - 0.041833''t^3 \\ z_A & = & 2306.2181''t + 1.09468''t^2 + 0.018203''t^3 \end{cases}$$

and the time t is defined as:

$$t = \frac{(TT - J2000.0)}{36525}$$

where TT is the Terrestrial Time (dd/mm/yyyy, hh:mm). The transformation matrix is then perfectly defined for a certain epoch

Mean of Date to True of Date

Besides the “long-term” precession motion, equinoxes suffer also short-period, small oscillations, which are denoted as nutations. For more clarity, see figure **PUT FIGURE NUTATION PRE-CESSION**. The True of Date (TOD) frame is thus defined as:

$$TOD \equiv \begin{cases} \text{X-axis} & \equiv & \text{Earth's COM} \longrightarrow \text{True vernal equinox at current epoch} \\ \text{Z-axis} & \equiv & \text{Perpendicular to the true equatorial plane at current epoch} \\ \text{Y-axis} & \equiv & \text{Perpendicular to the X and Z axes forming a right-handed system} \end{cases}$$

The rotation matrix now has the following shape:

$$R_{MOD \rightarrow TOD} = \begin{bmatrix} C\Delta\psi & -C\epsilon_m S\Delta\psi & -S\epsilon_m S\Delta\psi \\ C\epsilon_t S\Delta\psi & C\epsilon_m C\epsilon_t C\Delta\psi + S\epsilon_m S\epsilon_t & S\epsilon_m C\epsilon_t C\Delta\psi - C\epsilon_m S\epsilon_t \\ S\epsilon_t S\Delta\psi & C\epsilon_m S\epsilon_t C\Delta\psi - S\epsilon_m C\epsilon_t & S\epsilon_m S\epsilon_t C\Delta\psi + C\epsilon_m C\epsilon_t \end{bmatrix} \quad (B.2)$$

where four angles appear. Firstly, the mean obliquity, which is the angle between the mean ecliptic and the mean equatorial plane ($\approx 23.5^\circ$), whose value is computed by:

$$\epsilon_m = 84381.448'' - 46.8150''t - 0.00059''t^2 + 0.001813''t^3$$

Moreover, two nutations appear: the one in longitude and the one in obliquity ($\Delta\psi$ and $\Delta\epsilon$, respectively). These angles are computed by a summation of a large number of sinusoidal functions, whose construction and coefficients are shown in [11]. Lastly, the true obliquity is simply the addition of its mean counterpart and the nutation ($\epsilon_t = \epsilon_m + \Delta\epsilon$).

True of Date to Pseudo-Body-Fixed

Perhaps the biggest and most intuitive difference between ECI and ECEF is Earth's rotation around its axis. The pseudo-body-fixed is simply a clockwise rotation (seen from north pole towards the Earth's COM) around said axis from the True of Date frame:

$$PBF \equiv \left\{ \begin{array}{lll} \text{X-axis} & \equiv & \text{Earth's COM} \longrightarrow \text{Intersection between prime meridian and true equatorial plane} \\ & & \text{(without accounting for the axis' displacement).} \\ \text{Z-axis} & \equiv & \text{Perpendicular to the true equatorial plane at current epoch} \\ \text{Y-axis} & \equiv & \text{Perpendicular to the X and Z axes forming a right-handed system} \end{array} \right.$$

The rotation matrix is now as simple as:

$$R_{TOD \rightarrow PBF} = \begin{bmatrix} C\alpha_G & S\alpha_G & 0 \\ -S\alpha_G & C\alpha_G & 0 \\ 0 & 0 & 1 \end{bmatrix} \quad (\text{B.3})$$

where α_G is referred to as the Greenwich Mean Sidereal Time (GMST). $\dot{\alpha}_G$ is then the rotation rate of the Earth. An analytical expression for this angle is provided in [10], which is:

$$\begin{aligned} \text{GMST(UT1)} = & 4.894961212823058751375704430 \\ & + \Delta T \{ 6.300388098984893552276513720 \\ & + \Delta T (5.075209994113591478053805523 \times 10^{-15} \\ & - 9.253097568194335640067190688 \times 10^{-24} \Delta T) \} \end{aligned}$$

where $\Delta T = \text{UT1} - \text{J2000.0}$ is expressed in days (including the fractional part of a day).

Pseudo-Body-Fixed to Body-Fixed (ECEF)

The last, and surely most subtle transformation, is the one that accounts for the displacement in Earth's axis of rotation. This displacement is parametrized with the polar angles x_p and y_p , which can again be found at [11]. As these angles are sufficiently small, the rotation matrix from PBF to ECEF is:

$$R_{PBF \rightarrow BF} = \begin{bmatrix} 1 & 0 & x_p \\ 0 & 1 & -y_p \\ -x_p & y_p & 1 \end{bmatrix} \quad (\text{B.4})$$

Full rotation matrix $R_{ECI \rightarrow ECEF}$.

By simply successively composing rotations, the full rotation matrix from ECI to ECEF is computed

as:

$$R_{ECI \rightarrow ECEF} = R_{PBF \rightarrow ECEF} R_{TOD \rightarrow PBF} R_{MOD \rightarrow TOD} R_{ECI \rightarrow MOD}$$

B.2.3 Perifocal (PQW) reference frame.

B.2.3.1 Definition.

The perifocal reference frame is defined as:

$$PQW \equiv \left\{ \begin{array}{lll} \text{Origin} & \equiv & \text{Central body's COM} \\ \text{X-axis} & \equiv & \text{Origin} \longrightarrow \text{Periapsis.} \\ \text{Z-axis} & \equiv & \text{Perpendicular to the osculating orbital plane (out-of-plane)} \\ \text{Y-axis} & \equiv & \text{Perpendicular to the X and Z axes forming a right-handed system} \end{array} \right.$$

This frame takes advantage of the motion being contained in the orbital plane (when using osculating elements, see **CITE MEAN2OSC**). That means that usually, the problem reduces to evaluating two components of the position and velocity. It also allows for a quite straightforward description of the motion in terms of the Keplerian OEs, assuming elliptical motion. In this case, and using \underline{q} and $\underline{\dot{q}}$ to denote perifocal position and velocity, the perifocal state vector is expressed as:

$$\underline{q} = \begin{pmatrix} r \cos \theta \\ r \sin \theta \\ 0 \end{pmatrix} = \begin{pmatrix} a(\cos E - e) \\ a \sin E \\ 0 \end{pmatrix} \quad \underline{\dot{q}} = \frac{na}{\sqrt{1-e^2}} \begin{pmatrix} -\sin \theta \\ e + \cos \theta \\ 0 \end{pmatrix}$$

where E is the eccentric anomaly, r is the orbital radius, n is the mean orbital rate and the remaining parameters are the regular Keplerian OEs. r and n can be expressed as a function of them as:

$$r = \frac{a(1-e^2)}{1+e \cos \theta} = a(1-e \cos E) ; \quad n = \sqrt{\frac{\mu}{a^3}}$$

with $\mu = GM$ being the gravitational parameter of the central body.

B.2.3.2 State vector transformation.

Rotation matrix from & to ECI.

As done with the ECI to ECEF transformation, this one can also be decomposed in three rotations,

each associated with one Keplerian angle.

The first rotation is associated to Ω , being done around the Z ECI axis. The resulting frame will be named I1 (intermediate 1), and the rotation matrix from ECI is:

$$R_{ECI \rightarrow I1}(\Omega) = \begin{bmatrix} \cos \Omega & \sin \Omega & 0 \\ -\sin \Omega & \cos \Omega & 0 \\ 0 & 0 & 1 \end{bmatrix}$$

Afterwards, a rotation around X axis of I1 (nodal line) of value i is performed, leading to frame I2. The rotation matrix is simply:

$$R_{I1 \rightarrow I2}(\Omega) = \begin{bmatrix} 1 & 0 & 0 \\ 0 & \cos i & \sin i \\ 0 & -\sin i & \cos i \end{bmatrix}$$

Finally, a rotation around Z axis of I2 (out-of-plane direction) of value ω is done, yielding the desired perifocal frame (which we will denote as PQW):

$$R_{I2 \rightarrow PQW}(\Omega) = \begin{bmatrix} \cos \omega & \sin \omega & 0 \\ -\sin \omega & \cos \omega & 0 \\ 0 & 0 & 1 \end{bmatrix}$$

By composition, the matrix $R_{ECI \rightarrow PQW}$ can easily be calculated:

$$R_{ECI \rightarrow PQW} = R_{I2 \rightarrow PQW} R_{I1 \rightarrow I2} R_{ECI \rightarrow I1} = \begin{bmatrix} C\Omega C\omega - S\Omega CiS\omega & S\Omega C\omega + C\Omega CiS\omega & SiS\omega \\ -C\Omega S\omega - S\Omega CiC\omega & C\Omega CiC\omega + S\Omega S\omega & SiC\omega \\ S\Omega Si & -C\Omega Si & Ci \end{bmatrix}$$

Angular velocity.

In order to fully transform the system, it is necessary to calculate the relative angular velocity between both frames. Again, that can be done by composing the angular movements:

$$\underline{\omega}_{PQW \text{ w.r.t. } ECI} = \dot{\Omega} \underline{\hat{k}}_{I1} + \dot{i} \underline{\hat{k}}_{I2} + \dot{\omega} \underline{\hat{k}}_{PQW}$$

Expressing everything in PQW frame:

$$\underline{\omega}_{PQW \text{ w.r.t. } ECI}|_{PQW} = \begin{Bmatrix} \omega_x \\ \omega_y \\ \omega_z \end{Bmatrix} \dot{R}_{ECI \rightarrow PQW} \begin{Bmatrix} 0 \\ 0 \\ 1 \end{Bmatrix} + \dot{R}_{I2 \rightarrow PQW} R_{I1 \rightarrow I2} \begin{Bmatrix} 1 \\ 0 \\ 0 \end{Bmatrix} + \dot{R}_{I2 \rightarrow PQW} \begin{Bmatrix} 0 \\ 0 \\ 1 \end{Bmatrix}$$

In virtue of the axial dual form principle, there exists one matrix that, when applied to a certain vector, yields the same result as doing the cross product between $\underline{\omega}$ and that vector. This matrix has the following shape:

$$\Omega_{PQW \text{ w.r.t. } ECI}|_{PQW} = \begin{bmatrix} 0 & -\omega_z & \omega_y \\ \omega_z & 0 & -\omega_x \\ -\omega_y & \omega_x & 0 \end{bmatrix}$$

As the relative rotation of the opposite motion is just the opposite of the original, and applying a rotation:

$$\Omega_{ECI \text{ w.r.t. } PQW}|_{ECI} = -\Omega_{PQW \text{ w.r.t. } ECI}|_{ECI} = -R_{PQW \rightarrow ECI} \Omega_{PQW \text{ w.r.t. } ECI}|_{PQW}$$

This will be useful later on.

Transformation matrices $T_{PQW \rightarrow ECI}$, $T_{ECI \rightarrow PQW}$.

Let us consider the following coordinate transformation:

$$\underline{x}_{PQW} = R_{ECI \rightarrow PQW} \underline{x}_{ECI}$$

If we want then to also transform its time derivative, one option is to directly differentiate by parts with respect to time:

$$\dot{\underline{x}}_{PQW} = \dot{R}_{ECI \rightarrow PQW} \underline{x}_{ECI} + R_{ECI \rightarrow PQW} \dot{\underline{x}}_{ECI}$$

where the matrix $\dot{R}_{ECI \rightarrow PQW}$ can be either directly calculated term by term, or otherwise computed as:

$$\dot{R}_{ECI \rightarrow PQW} = \dot{R}_{ECI \rightarrow PQW} \Omega_{ECI \text{ w.r.t. } PQW}|_{ECI}$$

B.3 Relative reference systems.

B.3.1 LVLH reference frame.

B.3.1.1 Definition.

B.3.1.2 State vector transformation.

A) Using reference orbit's Keplerian OEs.

Rotation matrix from $\&$ to ECI.

Angular velocity.

Transformation matrices $T_{LVLH \rightarrow ECI}$, $T_{ECI \rightarrow LVLH}$.

B) Using reference ECI state vector.

Rotation matrix from $\&$ to ECI.

Angular velocity.

Transformation matrices $T_{PQW \rightarrow ECI}$, $T_{ECI \rightarrow PQW}$.

B.3.2 RTN reference frame.**B.3.2.1 Definition.****B.3.2.2 State vector transformation.**

Rotation matrix from & to ECI.

Angular velocity.

Transformation matrices $T_{RTN \rightarrow ECI}$, $T_{ECI \rightarrow RTN}$.

B.3.3 TAN reference frame.**B.3.3.1 Definition.****B.3.3.2 State vector transformation.**

Rotation matrix from & to LVLH.

Angular velocity.

Transformation matrices $T_{TAN \rightarrow LVLH}$, $T_{LVLH \rightarrow TAN}$.

B.4 Conversions from OEs to cartesian coordinates.**B.4.1 ECI to Keplerian OEs and vice versa.****B.4.2 Relative Keplerian OEs to LVLH.**

Bibliography

General

Books

- [1] W. E. Wiesel. MODERN ASTRODYNAMICS. 2nd ed. Beaver Creek, Ohio: Aphelion Press, 2010 (cit. on pp. [2](#), [3](#)).
- [9] P. K. S. Dennis D. McCarthy. TIME: FROM EARTH ROTATION TO ATOMIC PHYSICS. Wiley-VCH, 2009. ISBN: 3527407804; 9783527407804 (cit. on pp. [14](#), [15](#)).
- [10] B. D. Tapley, B. E. Schutz, and G. H. Born. STATISTICAL ORBIT DETERMINATION. 1st ed. Amsterdam, Netherlands: Elsevier, 2004.
- [12] O. Montenbruck and E. Gill. SATELLITE ORBITS: MODELS, METHODS AND APPLICATIONS. 1st ed. Wessling, Germany: Springer, 2001.
- [13] K. T. Alfriend and Srinivas. SPACECRAFT FORMATION FLYING. 1st ed. Oxford, United Kingdom: Elsevier, 2010.
- [14] R. H. Battin. AN INTRODUCTION TO THE MATHEMATICS AND METHODS OF ASTRODYNAMICS, REVISED EDITION. 1st ed. Reston, Virginia: American Institute of Aeronautics and Astronautics, 1999.
- [15] D. Brouwer and G. M-Clemence. METHODS OF CELESTIAL MECHANICS. Brackley Square House, London: Academic Press, 1961.
- [16] H. Schaub and J. L. Junkins. ANALYTICAL MECHANICS OF SPACE SYSTEMS. Reston, VA: AIAA Education Series, Oct. 2003. DOI: [10.2514/4.861550](#).

Articles

- [6] H. Schaub. RELATIVE ORBIT GEOMETRY THROUGH CLASSICAL ORBIT ELEMENT DIFFERENCES. In: *Journal of Guidance, Control & Dynamics* 27.5 (2004), pp. 839–848. DOI: [10.2514/1.12595](#) (cit. on pp. [5](#), [9](#), [10](#)).
- [19] J. Sullivan, S. Grimberg, and S. D’Amico. COMPREHENSIVE SURVEY AND ASSESSMENT OF SPACECRAFT RELATIVE MOTION DYNAMICS MODELS. In: *Journal of Guidance, Control & Dynamics* 40.8 (2017), pp. 1837–1859. DOI: [10.2514/1.G002309](#).

- [20] N. Capitaine. THE CELESTIAL POLE COORDINATES. In: *Celestial Mechanics and Dynamical Astronomy* 48 (1990), pp. 127–143.

Eccentric Dynamics

Articles

- [2] M. Eckstein, C. Rajasingh, and P. Blumer. COLOCATION STRATEGY AND COLLISION AVOIDANCE FOR THE GEOSTATIONARY SATELLITES AT 19 DEGREES WEST. In: *CNES International Symposium on Space Dynamics*. Vol. 25. Oberpfaffenhofen, Germany: DLR GSOC, Nov. 1989, pp. 60–66 (cit. on pp. 3, 4).
- [3] S. D’Amico and O. Montenbruck. PROXIMITY OPERATIONS OF FORMATION-FLYING SPACECRAFT USING AN ECCENTRICITY/INCLINATION VECTOR SEPARATION. In: *Journal of Guidance, Control & Dynamics* 29.3 (2006), pp. 554–563. DOI: [10.2514/1.15114](https://doi.org/10.2514/1.15114) (cit. on pp. 4, 9, 11).
- [8] T. Vincent Peters and R. Noomen. LINEAR COTANGENTIAL TRANSFERS AND SAFE ORBITS FOR ELLIPTIC ORBIT RENDEZVOUS. In: *Journal of Guidance, Control & Dynamics* 44.4 (2021), pp. 732–748. DOI: [10.2514/1.G005152](https://doi.org/10.2514/1.G005152) (cit. on pp. 11, 12).
- [21] K. Yamanaka and F. Ankersen. NEW STATE TRANSITION MATRIX FOR RELATIVE MOTION ON AN ARBITRARY ELLIPTICAL ORBIT. In: *Journal of Guidance, Control & Dynamics* 25.1 (2002), pp. 60–66. DOI: [10.2514/2.4875](https://doi.org/10.2514/2.4875).
- [22] R. Broucke. ON THE MATRIZANT OF THE TWO-BODY PROBLEM. In: *Astronomy and Astrophysics* 6 (June 1970), p. 173.

Perturbations

Books

- [17] A. H. Nayfeh. PERTURBATION METHODS. Weinheim, Germany: Wiley-VCH, 2004.
- [18] W. M. Kaula. THEORY OF SATELLITE GEODESY. Mineola, New York: Dover Publications, 2013.

Articles

- [4] D.-W. Gim and K. T. Alfriend. SATELLITE RELATIVE MOTION USING DIFFERENTIAL EQUINOCTIAL ELEMENTS. In: *Celestial Mechanics and Dynamical Astronomy* 92.4 (2005), pp. 295–336. DOI: [10.1007/s10569-004-1799-0](https://doi.org/10.1007/s10569-004-1799-0) (cit. on p. 5).
- [5] S. D’Amico. RELATIVE ORBITAL ELEMENTS AS INTEGRATION CONSTANTS OF HILL’S EQUATIONS. TN 05-08. Deutsches Zentrum für Luft- und Raumfahrt (DLR), 2005 (cit. on pp. 5, 9).
- [7] G. Gaias, C. Colombo, and M. Lara. ACCURATE OSCULATING/MEAN ORBITAL ELEMENTS CONVERSIONS FOR SPACEBORNE FORMATION FLYING. In: (Feb. 2018). https://www.researchgate.net/publication/340378956_Accurate_Osculating_Mean_Orbital_Elements_Conversions_for_Spaceborne_Formation_Flying (cit. on p. 6).
- [23] D.-W. Gim and K. Alfriend. STATE TRANSITION MATRIX OF RELATIVE MOTION FOR THE PERTURBED NONCIRCULAR REFERENCE ORBIT. In: *Journal of Guidance Control and Dynamics* 26 (Nov. 2003), pp. 956–971. DOI: [10.2514/2.6924](https://doi.org/10.2514/2.6924).
- [24] G. Gaias, J.-S. Ardaens, and C. Colombo. PRECISE LINE-OF-SIGHT MODELLING FOR ANGLES-ONLY RELATIVE NAVIGATION. In: *Advances in Space Research* 67.11 (2021). Satellite Constellations and Formation Flying, pp. 3515–3526. DOI: [10.1016/j.asr.2020.05.048](https://doi.org/10.1016/j.asr.2020.05.048).
- [25] G. Gaias, C. Colombo, and M. Lara. ANALYTICAL FRAMEWORK FOR PRECISE RELATIVE MOTION IN LOW EARTH ORBITS. In: *Journal of Guidance, Control, and Dynamics* 43.5 (2020), pp. 915–927. DOI: [10.2514/1.G004716](https://doi.org/10.2514/1.G004716).
- [26] D. Brouwer. SOLUTION OF THE PROBLEM OF ARTIFICIAL SATELLITE THEORY WITHOUT DRAG. In: *Astronomical Journal* 64.5 (Nov. 1959), p. 378. DOI: [10.1086/107958](https://doi.org/10.1086/107958).
- [27] R. H. Lyddane. SMALL ECCENTRICITIES OR INCLINATIONS IN THE BROUWER THEORY OF THE ARTIFICIAL SATELLITE. In: *Astronomical Journal* 68 (Oct. 1963), p. 555. DOI: [10.1086/109179](https://doi.org/10.1086/109179).

Matlab Exchange libraries

- [28] F. G. Nievinski. SUBTIGHTPLOT. <https://www.mathworks.com/matlabcentral/fileexchange/39664-subtightplot>. 2013.
- [29] J. C. Lansey. LINSPECER. <https://www.mathworks.com/matlabcentral/fileexchange/42673-beautiful-and-distinguishable-line-colors-colormap>. 2015.

-
- [30] Jan. WINDOWAPI. <https://www.mathworks.com/matlabcentral/fileexchange/31437-windowapi>. 2013.
 - [31] T. Davis. ARROW3. <https://www.mathworks.com/matlabcentral/fileexchange/14056-arrow3>. 2022.